

# Flux creep in type-II superconductors: self-organized criticality approach

R.G. Mints\* and Ilya Papiashvili

*School of Physics and Astronomy, Raymond and Beverly Sackler  
Faculty of Exact Sciences, Tel Aviv University, Tel Aviv 69978, Israel*

(Dated: November 14, 2018)

We consider the current density distribution function of a flux creep regime in type-II superconductors by mapping the flux creep process to the dynamics of a model with a self-organized criticality. We use an extremal Robin Hood type model which evolves to Been's type critical state to treat magnetic flux penetration into a superconductor and derive an analog of the current-voltage characteristics in the flux creep region.

PACS numbers: 74.60. Ec, 74.60. Ge

## I. INTRODUCTION

In the presence of currents vortex structure in a type-II superconductor is subjected to Lorentz force. The value of this force per unit length of a vortex is  $\mathbf{f}_L = \mathbf{j} \times \vec{\phi}_0$ , where  $\mathbf{j}$  is the current density,  $\mathbf{B}$  is the magnetic field,  $\vec{\phi}_0 = \phi_0 \mathbf{B}/B$ , and  $\phi_0$  is the flux quantum. The Lorentz force acting on a unit volume of a vortex matter is therefore given by  $\mathbf{F}_L = n \mathbf{f}_L = \mathbf{j} \times \mathbf{B}$ , where  $n(\mathbf{r}) = B(\mathbf{r})/\phi_0$  is the density of the vortices<sup>1,2</sup>.

Consider as an illustration a superconducting slab parallel to the  $y, z$ -plane and assume that a certain magnetic field  $B_a$  is applied along the  $z$ -axis as shown in Fig. 1. In this case we have  $\mathbf{j} = j \hat{y}$  and  $\mathbf{B} = B \hat{z}$  related by Maxwell's equation  $dB/dx = -\mu_0 j$ . The Lorentz force  $F_L = jB$  is therefore proportional to the density of vortices  $n$  and its gradient  $dn/dx$  as follows from  $F_L = jB \propto B dB/dx \propto n dn/dx$ .

In high-current density superconductors defects of the crystalline structure "pin" the vortices. This pinning leads to creation of various vortex configurations with flux "hills" and flux "valleys" between these hills. Indeed, single vortices or bundles of vortices redistribute spatially if the Lorentz force  $F_L \propto j \propto dn/dx$  overcomes the pinning force  $F_{\text{pin}}$ . This means that  $n dn/dx \propto F_{\text{pin}}$ , *i.e.*, a steady vortex structure consists of a composition of fragments with a certain slope  $dn/dx \neq 0$  (the flux hills). On a macroscopic level we have  $F_L \propto j$  and therefore the local depinning of vortices happens when the local current density  $j$  exceeds a certain *critical* value  $j_c \propto F_{\text{pin}}$ . It was pointed out by de Gennes that the flux hills with slopes statistically fixed by the critical current density  $j_c$  are very much alike to the sand piles<sup>1</sup>.

The concept of approaching to flux statics and dynamics in superconductors with high density of pinning centers was first suggested by Been<sup>3</sup>. The famous Bean's model assumes that the current density  $j$  is equal to the critical current density  $j_c$  everywhere where there are currents. Initially Been considered a magnetic field independent  $j_c$ . As a result the spatial increase or decrease of the field inside the sample is linear. In particular, in a slab with thickness  $2d$  (see Fig. 1) the assumption  $j_c = \text{Const}$  leads to  $B = B_a - \mu_0 j_c |x \mp d|$ , where  $B_a$  is the mag-

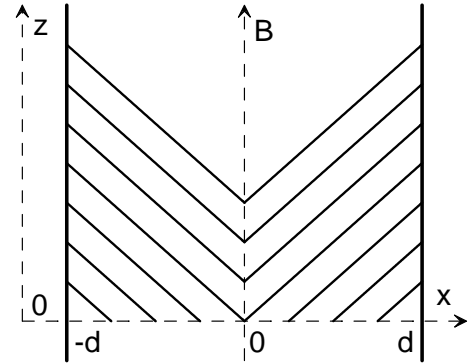


FIG. 1: Series of Been's critical states in a slab parallel to the  $yz$ -plane. A zero-field cooled sample was subjected to a monotonically increased field parallel to the  $z$ -axis. The slope of  $B(x)$  is proportional to the critical current density  $j_c$ .

netic field at the sample surface. In general, the field dependence of  $j_c$  has to be taken into account in order to give a better description of the whole wealth of the experimental data available<sup>4,5</sup>.

In this paper we treat the low-temperature flux creep in type-II superconductors in the framework of the self-organized criticality approach<sup>6,7,8,9,10,11,12,13,14,15,16</sup>. The distribution function of the current density  $j$  is considered in detail for an extremal Robin Hood type process<sup>9</sup>. We show that this process results in a self-organized Been's type critical state with a complex dynamics, which can be mapped to the low-temperature flux creep. This mapping is used to obtain an analog of a current-voltage characteristics of a type-II superconductors in the flux creep regime.

The paper is organized as follows. In Sec. II we discuss the dynamics of the low-temperature flux creep regime in type-II superconductors. The self-organized criticality of an extremal Robin Hood type process is treated in Sec. III. In Sec. IV we introduce the low-temperature flux creep model and derive the distribution function of the current density  $j$ . The magnetic flux penetration into a superconductor and an analog of current-voltage characteristics of a type-II superconductor in the flux creep regime are treated in Sec. V. Sec. VI summarizes the ob-

tained results.

## II. FLUX CREEP IN SUPERCONDUCTORS

There are few mechanisms resulting in depinning of vortices for currents with a density less than the critical value. In particular, both thermally activated depinning and quantum tunnelling<sup>4,17</sup> result in vortices and bundles of vortices jumping from one group of pinning centers to another. This type of vortex motion is called flux creep<sup>18</sup>. The probability of depinning of a bundle of vortices strongly depends on the current density and tends to unity when the current density tends to the critical current density, *i.e.*,  $j \rightarrow j_c$ . The high level of correlations between vortices in a vortex matter leads to a very complicated collective behavior of vortices especially in thin superconducting films where the stray fields result in nonlocality of the problem<sup>19</sup>. Activation of one vortex can ignite a local avalanche-type motion of bundles of correlated vortices, *i.e.*, in the flux creep region vortex matter is a system with avalanche driven dynamics. Such systems with avalanche driven dynamics are the subject of the modern theory of self-organized criticality which revealed a variety of power-law distributions for the spatial size and temporal duration of the avalanches<sup>6,7</sup>.

Motion of vortices is accompanied by the field and current energies dissipation. The heat release during rearrangements (flux avalanches) in a vortex matter can heat up the whole sample or a part of it to a temperature higher than the critical temperature  $T_c$ . Under certain conditions an avalanche of even a small group of vortices can trigger a run-away magneto-thermal instability causing the superconducting-to-normal transition<sup>20</sup>.

The original Bean's model means that in the critical state the dependence of  $j$  on  $E$  is a highly nonlinear step-wise function

$$\mathbf{j} = \mathbf{j}_c \begin{cases} 0, & \text{if } E = 0, \\ 1, & \text{if } E \neq 0, \end{cases} \quad (1)$$

where  $\mathbf{j}_c = j_c \hat{\mathbf{e}}$  and  $\hat{\mathbf{e}} = \mathbf{E}/E$  is a unit vector parallel to the electric field  $\mathbf{E}$  induced by flux motion.

It is well established now that in the narrow vicinity of the critical current ( $|j - j_c| \ll j_c$ ), *i.e.*, in the flux creep regime the dependence of  $j$  on  $E$  is a very steep function given by the power law

$$\mathbf{j} = \mathbf{j}_c \left( \frac{E}{E_0} \right)^{1/n}, \quad (2)$$

where  $n \gg 1$  is a parameter and the field  $E_0$  defines the critical current density. It is common to define  $j_c$  as the current density at  $E_0 = 10^{-6}$  Vcm<sup>-1</sup>. It is worth mentioning that for  $n \gg 1$  we can rewrite Eq. (2) in the following logarithmic form

$$\mathbf{j} = \mathbf{j}_c + \frac{\mathbf{j}_c}{n} \ln \left( \frac{E}{E_0} \right), \quad (3)$$

where the omitted terms are of order  $1/n^2 \ll 1$ .

The dependence of  $j$  on  $E$  given by Eq. (2) was first derived in the framework of the Anderson-Kim model<sup>5</sup> considering the thermally activated uncorrelated hopping of bundles of vortices. The vortex-glass<sup>21</sup> and collective creep<sup>22,23</sup> models result in more sophisticated dependencies of  $j$  on  $E$ . However, these dependencies coincide with the one given by Eq. (2) if  $j - j_c \ll j_c$ . The recently developed self-organized criticality approach to the critical state<sup>10,11</sup> also leads to Eq. (2) if  $j - j_c \ll j_c$ . In the interval  $j - j_c \ll j_c$  the power law (2) is in good agreement with numerous experimental data<sup>24</sup>.

A detailed study of the dynamics of vortices in the flux creep regime was performed by Field and coworkers<sup>12</sup>. In their experiments the magnetic field outside a tubular superconducting sample is ramped slowly, driving the flux into the tubes outer wall. After the flux front reaches the inner wall of a tube it spills out into the tube's interior. The entrance of flux into the tube's interior was detected in real time. This experiment distinguished between flux leaving the superconductor in discrete bundles or avalanches. It was shown that the probability  $D(s)$  of an avalanche containing  $s$  vortices is a power-law dependence extending over 1.6 decades.

Been's critical state dynamics is typical to some other spatially extended dynamical systems. High number of degrees of freedom in these systems introduces the problem of treating the effect of coupling between the individual degrees of freedom. In many cases even very complicated systems "self-organize" so that their description reduces to a small number of collective degrees of freedom<sup>6,7</sup>.

In some dynamical systems the individual degrees of freedom keep each other in a stable balance, which cannot be described as a "perturbation" of some decouple state as well as in terms of a small amount of collective degrees of freedom. This type of the self-organized systems has to be quite robust. In the opposite case these systems would not be able to evolve to a stable balanced "critical" state<sup>6,7</sup>. The sand piles and flux hills in superconductors demonstrate many features typical for the self-organized critical state.

Several different models were suggested to illustrate and study dynamical systems with extended spatial degrees of freedom and many metastable states. These systems evolve into a *self-organized* critical state without a detailed specification of the initial conditions, *i.e.*, the critical state is an attractor of their dynamics which is robust with respect to variations of parameters and the presence of quenched randomness.

## III. SELF-ORGANIZED CRITICALITY OF EXTREMAL PROCESSES

We consider now a specific subclass of *extremal* processes demonstrating the self-organized criticality. In extremal models at each step only the sites satisfying a

certain extremal criterion are involved into the system dynamics. In particular, the problem of low-temperature flux creep in superconductors can be mapped to the Robin Hood type extremal model<sup>9</sup>.

### A. Robin Hood processes.

The following picture illustrates the main idea of the Robin Hood type process. The famous robber leaves everyday his forest for a nearest market and tries to obtain justice. He finds the richest seller, takes from him some random amount of goods or money and distributes it among neighbors. He takes nothing to himself so that overall amount of goods on the market is conserved. The market reaches a critical state after some transition time.

Many physical systems with a dynamical variable matching a certain conservation relation can be treated in the framework of the Robin Hood model. In particular, the low-temperature flux creep, motion of dislocations through a random array of point obstacles, domain walls in ferromagnets, grain boundaries in polycrystals, *etc.* can be mapped to this type of extremal processes<sup>9</sup>. We will use the Robin Hood type model to treat the self-criticality of the low-temperature flux creep in superconductors in detail.

### B. Low-temperature flux creep

If the temperature is very low than vortices in sites with even slightly different current density have strongly different probability of depinning. Therefore, the depinning of vortices will happen first in the place with the highest current density.

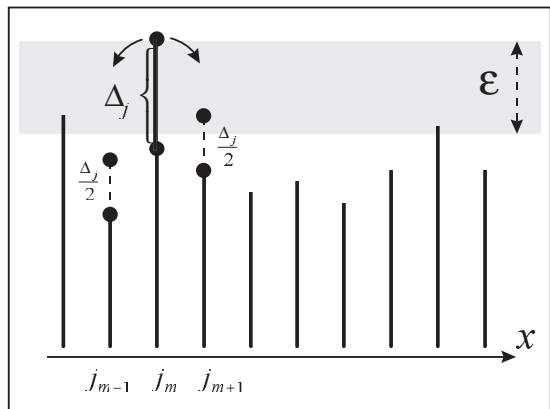


FIG. 2: Illustration of the dynamics rules of the Robin Hood type low-temperature flux creep model.

The model suggested by Zaitsev<sup>9</sup> simulates a part of a superconductor with  $L$  sites using the closed boundary conditions. Numbers  $j_i$  ( $0 \leq i \leq L$ ) describe the values of the current density  $j$  along the  $x$ -axis (the current flows

along the  $y$ -axis). At each simulation step a site number  $m$  with the maximal current density  $j_m$  is found (see Fig. 2). This current density is reduced by  $\Delta_j$  chosen from a uniform distribution  $U(j)$

$$j_m \rightarrow j_m - \Delta_j, \quad j_{m\pm 1} \rightarrow j_{m\pm 1} + \Delta_j/2. \quad (4)$$

It is worth mentioning that Zaitsev's model conserves the total current

$$I = \sum_{n=1}^L j_n = \langle j \rangle L, \quad (5)$$

which means that the average value of the critical current density  $\langle j \rangle$  is also conserved. The system approaches the critical state starting from any initial state with a given value of  $\langle j \rangle$ . In this critical state almost all sites have current densities less than a certain value  $j_c$ . Each site of the system maps an area in a superconductor containing a large amount of vortices but depinning is referred to a single vortex. Motion of this vortex leads to a rearrangement of a cluster of correlated vortices and changes the local current density by some value which is determined by the uniform distribution  $U(j)$ .

The distribution of the values of  $\Delta_j$  which will be referred below as  $\Delta_j$ -distribution, defines the number of vortices participating in an avalanche starting from a depinning of a single vortex, or, to be more precise, it is related to the number of vortices leaving a given site as a result of an avalanche. At sufficiently low temperature this vortex rearrangement is a very fast process comparing to the thermally activated depinning. Therefore, all the details concerning these avalanches, including microscopic vortex dynamics, are "hidden" in  $\Delta_j$ -distribution.

### C. Dynamics of extremal processes

The fact that the flux creep dynamics conserves the total current  $I$  leads to a high level of correlation between the sites. In the extremal models the extremal sites are located according to some problem-specific criterion and they provoke changes of the neighbor sites, again, according to rules specific for a given model. We will call these sites *ignition* sites. The sites drawn in the activity by the ignition sites will be called *involved* sites. An involved site in its order can become an ignition site if it matches a certain extremal criterion. A system in a critical state is characterized by a critical value of the dynamical parameter. In particular, for the flux creep model this parameter is  $j_c$  which is the least value of  $j$  in the ignition sites. That means that for the flux creep model all ignition sites have values greater than  $j_c$ .

The rules of dynamics given by Eq. (4) are illustrated schematically in Fig. 3. The interval of values of current densities in the ignition sites we call *active zone*. Each site in the active zone, *active site*, at a certain moment becomes an ignition site. At any step only a small part of all sites is active. As shown in Fig. 3 the majority of

the sites belongs to the *calm* zone. We will consider the dynamical properties of the low-temperature creep model (4) using this terminology.

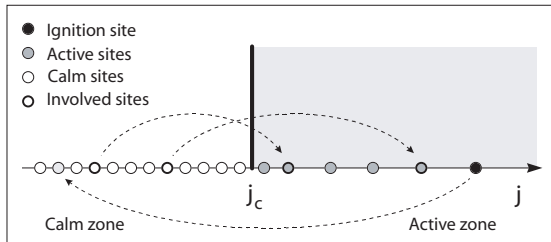


FIG. 3: The calm and the active zones for a one-dimensional flux creep model. The rules of dynamics given by Eq. (4) are illustrated by the dashed lines.

#### IV. LOW TEMPERATURE CREEP MODEL

The results of our numerical simulations of a system obeying the dynamics rules given by Eq. (4) demonstrate that  $G(j)$  is described by an exponent up to a certain critical value  $j_c$ , *i.e.*,

$$G(j) = A \exp(j/j_e), \quad \text{for } j_c - 1 < j < j_c, \quad (6)$$

where  $A$  and  $j_e$  are parameters of the distribution (see Fig. 4). The distribution function  $G(j)$  has a sharp cut off at  $j = j_c$ . In the active zone ( $j > j_c$ ) the “tail” of  $G(j)$  decreases as  $1/L$ , when  $L \rightarrow \infty$  (see Fig. 5).

The distribution function  $G(j)$  has another cut off at  $j_c - 1$  if the  $\Delta_j$ -distribution in the interval  $(0, 1)$  is chosen to be uniform. Indeed, there are only two options to create a site with a current density  $j$ : (a) to decrease the current density in the ignition site by  $\Delta_j$  and (b) to increase the current density in one of the involved sites by  $\Delta_j/2$ . The lowest value of  $j$  is obtained by subtracting from the minimum value of the current density in an ignition site, which is  $j_c$ , the maximum value from  $U$ , which is 1. As a result the distribution function  $G(j)$  has a cut off from the left. This cut off is not universal and depends on the  $\Delta_j$ -distribution. A continuously decreasing  $\Delta_j$ -distribution eliminates both the left cut off and the deviation of  $G(j)$  from the exponential function in the vicinity of  $j_c$ . The details of a specific  $\Delta_j$ -distribution affect only the tail of the function  $G(j)$ , *i.e.*, its behavior in the interval  $j > j_c$ . Therefore, we conclude that the values of the current density  $j$  are distributed according to the exponential law given by Eq. (6) in almost all sites of the system.

##### A. Relation between the parameter $j_e$ and $j_c$

The relation between the parameter  $j_e$  and the critical current density  $j_c$  can be calculated analytically using the

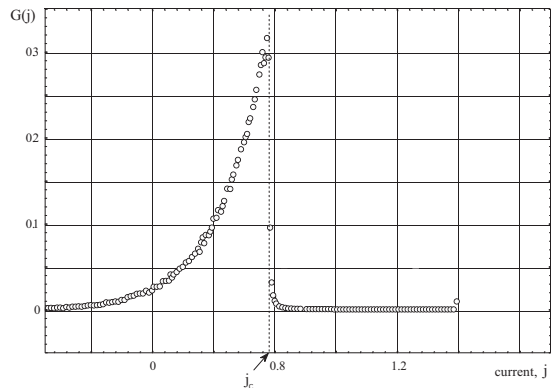


FIG. 4: The dependence of the distribution function  $G(j)$  on the current density  $j$ .

normalization and average current density conservation rules. Indeed, normalization of the distribution function  $G(j)$  given by Eq. (6)

$$\int_{-\infty}^{j_c} G(j) dj = A \int_{-\infty}^{j_c} \exp(j/j_e) dj = 1 \quad (7)$$

relates  $A$ ,  $j_c$ , and  $j_e$

$$A = \frac{1}{j_e} \exp(-j_c/j_e). \quad (8)$$

Next, we calculate the average value of the current density

$$\langle j \rangle = \int_{-\infty}^{j_c} j G(j) dj \quad (9)$$

and obtain the dependence of  $A$ ,  $j_c$ , and  $j_e$  on  $\langle j \rangle$

$$\langle j \rangle = A j_e^2 (j_c/j_e - 1) \exp(j_c/j_e). \quad (10)$$

Combining Eqs. (8) and (10) we find the relation between the critical current density  $j_c$ , parameter of the exponent  $j_e$ , and average current density  $\langle j \rangle$

$$j_c - j_e = \langle j \rangle. \quad (11)$$

If  $\Delta_j$ -distribution is uniform, then we have  $\langle j \rangle = 1/2$  and we find

$$j_c - j_e = 1/2. \quad (12)$$

Our numerical simulations show that the exponential form (6) of the distribution function  $G(j)$  is universal, meaning that it does not depend on the spatial dimension of the model, on the form of the  $\Delta_j$ -distribution, on the dynamic rules of redistribution of  $\Delta_j$  between neighbors, and on the decision on how many sites from the vicinity of an ignition site are involved in the redistribution process (for example, next nearest neighbors can be included into the dynamics). Therefore, we conclude that the exponential behavior of  $G(j)$  is typical for extremal models with short range interactions and a conservation relation for the dynamical variable.

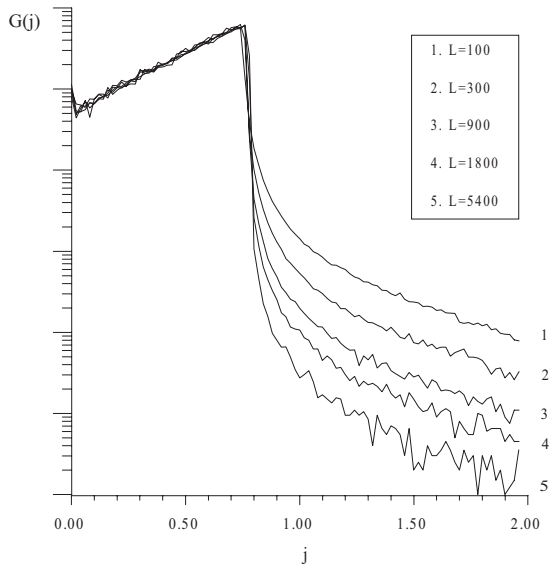


FIG. 5: Distribution functions  $G(j)$  for different values of the length of the system  $L$  in the region  $j > j_c$  [“tails” of  $G(j)$ ].

### B. Origin of the exponent

We performed numerical simulations for different extremal models and obtained the  $G(j)$  distribution for all of them. In addition to the uniform distribution for  $\Delta_j$  we tested also the exponential, gaussian, and power law distributions. These  $\Delta_j$ -distributions are more “natural” than  $U(j)$ , since they decay gradually and have no cut-offs, unlike the uniform distribution. All of them lead to the exponential form of  $G(j)$  if two conditions are satisfied. (a) Interactions in the model are local, meaning that an activated site affects only sites in its surrounding of a finite size; (b) At each step the sum of the dynamical variables ( $j_i$ ) stays constant.

The exponential behavior of  $G(j)$  can be obtained analytically as the most probable distribution of the dynamical variable  $j_i$ . To simplify the derivation we use discrete values of  $j$  dividing the whole interval of values of  $j$  into small intervals. In this case each site is characterized by a certain value  $j_i$ . We denote the number of sites with the same value  $j_i$  as  $n_i$  and write the conservation relations in the form

$$\sum_i n_i = L, \quad \sum_s n_i j_i = \langle j_i \rangle L. \quad (13)$$

Distribution of  $L$  sites between the intervals with  $j = j_i$  is described by a set  $\{n_i\}$  of numbers of sites in each interval. The number of states corresponding to the same set  $\{n_i\}$  is given by

$$\Gamma = \frac{L!}{\prod_i n_i!}. \quad (14)$$

Using Stirling’s formula we have for  $\sigma = \ln \Gamma$

$$\sigma = L \ln L - \sum_i n_i \ln n_i \quad (15)$$

The maximum of  $\sigma$  can be found using Lagrange method for conditional extremum with two conditions (13)

$$\begin{aligned} F &= \sigma + (\alpha + 1)L - \beta \langle j \rangle L \\ \frac{\partial F}{\partial n_i} &= -\ln n_i + \alpha + \beta j_i = 0 \end{aligned} \quad (16)$$

and we get finally

$$n_i = e^{\alpha + \beta j_i} \quad (17)$$

with  $\alpha$  and  $\beta$  defined by

$$\sum_i e^{\alpha + \beta j_i} = L, \quad \sum_i j_i e^{\alpha + \beta j_i} = \langle j \rangle L. \quad (18)$$

Using the continuous form of Eq. (18)

$$\int e^{\alpha + \beta j} = L, \quad \int j e^{\alpha + \beta j} dj = \langle j \rangle L \quad (19)$$

we find

$$\beta = \frac{1}{j_e}, \quad e^\alpha = A = \frac{1}{j_e} \exp(-j_c/j_e), \quad (20)$$

*i.e.*, the values  $j_c$ ,  $j_e$ , and  $\langle j \rangle$  are related by Eq. (11) and

$$G(j) = \frac{1}{j_e} \exp\left(\frac{j - j_c}{j_e}\right) = \frac{1}{e j_e} \exp\left(\frac{j - \langle j \rangle}{j_e}\right). \quad (21)$$

The distribution function given by Eq. (21) contains only one independent parameter,  $j_e$  which is characterizing the width of the distribution function  $G(j)$ . The value of  $j_e$  is proportional to the width  $\delta\Delta_j$  of the  $\Delta_j$ -distribution ( $j_e \propto \delta\Delta_j$ ) and depends, in particular, on the spatial dimension of the model, on the number of the neighbors of the ignition site, etc.

It is worth mentioning that the main features of the distribution function  $G(j)$  can be formulated in terms of a certain effective “temperature” associated with the system. Indeed, the above derivation of the distribution function  $G(j)$  is based on the same arguments which are used to derive the Gibbs distribution for a system of non-identical particles. We can write Eq. (21) in the form  $G(j) = \exp(-\epsilon_j/\tau)/j_e$ , where the effective “energy”  $\epsilon_j$  and “temperature”  $\tau$  are defined as  $\epsilon_j = a(j_c - j)$  and  $\tau = \alpha j_e$  and  $a$  is an arbitrary coefficient. Using Eq. (11) we find for the average energy

$$\langle \epsilon_j \rangle = a(j_c - \langle j \rangle) = \alpha j_e = \tau. \quad (22)$$

The value of the parameter  $j_e$  is proportional to the width  $\delta\Delta_j$  of the  $\Delta_j$ -distribution, and therefore the effective temperature  $\tau \propto \delta\Delta_j$ .

## V. FLUX PENETRATION MODEL

Extremal models can be useful for studying macroscopic processes in superconductors and, in particular, the process of penetration of magnetic flux. In this section we modify our model to allow for considering this process. The periodic boundary conditions which we used above simulated an inner part of the system located far from the sample edges.

Consider now a slab subjected to a magnetic field parallel to its surface as shown in Fig. 1. The symmetry of the problem allows to perform the numerical simulations in one half of the sample. Assume that the applied field rises up with a certain rate  $\dot{h}$  and the flux penetrates inside the sample from its left ( $x = -d$ ) edge. In this case the boundary condition at  $x = -d$  takes the form

$$j_0(t + \delta t) = j_0(t) + h \delta t, \quad (23)$$

where  $j_0(t)$  is the current density at  $x = -d$ .

The dynamics rule at the middle of the slab ( $x = 0$ ) has the form

$$\begin{aligned} j_L(t + \delta t) &= j_L(t) - \Delta_j, \\ j_{L-1}(t + \delta t) &= j_{L-1}(t) + \Delta_j/2, \end{aligned} \quad (24)$$

where  $j_L(t)$  is the current density at  $x = 0$ . It is worth mentioning that there is no current conservation at the sample boundaries at each simulation step. However, in a stationary state the current conservation holds in average for large time intervals.

### A. Introduction of the “real” time scale

The above self-organized criticality approach to the process of the low-temperature flux creep formulates the dynamical rules of the current density dynamics and operates with the simulation steps only. These steps correspond to the sequential depinning events in the process of numerical simulation of the model. The “real” time elapsed between two successive steps in the numerical simulations can vary significantly. This time mismatch has to be taken into consideration in order to relate the results of the calculations and experiments.

The temporal variation of the applied magnetic field has its own time-scale, which has to be synchronized with the “inner clock” of the numerical simulations. This synchronization can be done by calculating the “real” time interval between two successive depinning events. The extremal models of the low-temperature creep are based on the assumption that the depinning probability  $P_d$  strongly depends on the maximal current density  $j_m$  since the higher is  $j_m$  the higher is the depinning probability. We assume that this dependence has the “natural” exponential form

$$P_d \propto \exp\left[\frac{j_m - j_c}{j_1}\right] \propto \exp\left[\frac{j_m}{j_1}\right], \quad \text{for } j_m < j_c. \quad (25)$$

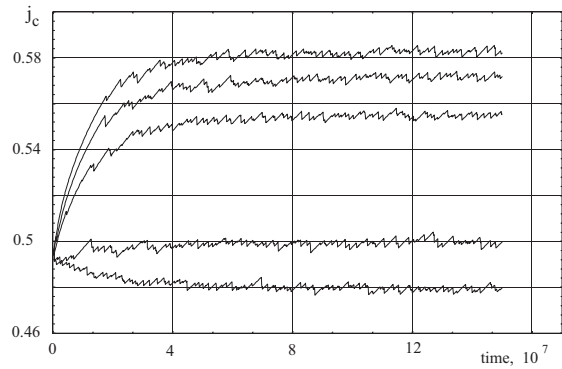


FIG. 6: Starting from the same initial distribution, the current density approaches different asymptotic values depending on the ramp rate  $h = 4 \times 10^{-5}$ ,  $3 \times 10^{-5}$ ,  $2 \times 10^{-5}$ ,  $5 \times 10^{-6}$ ,  $3 \times 10^{-6}$  (from top to bottom).

The mean time between two depinning events  $\langle \delta t \rangle$  is inversely proportional to  $P_d$  and therefore we write

$$\langle \delta t \rangle(t) = \delta t_{\text{tick}} \exp\left[-\frac{j_m(t)}{j_1}\right], \quad (26)$$

where  $\delta t_{\text{tick}}$  is the time interval corresponding to one *tick* of the “real” time clock. The last equation provides a synchronization mechanism between the steps in the numerical simulations and the “real” time intervals.

Using Eqs. (23) and (26) we arrive to the synchronized boundary condition at  $x = -d$  in the form

$$j_0(t + \delta t) = j_0(t) + h \delta t_{\text{tick}} \exp\left[-\frac{j_m(t)}{j_1}\right]. \quad (27)$$

Changing the time scale, so that  $h \delta t_{\text{tick}} \rightarrow h$  we rewrite Eq. (27) in the form convenient for recursive calculations

$$j_0 \rightarrow j_0 + h \exp\left[-\frac{j_m}{j_1}\right]. \quad (28)$$

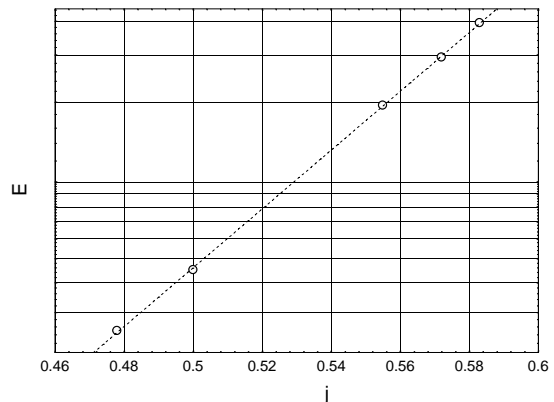


FIG. 7: Analogue of the current-voltage characteristics.

We treat now an analog of the  $j$ - $E$  curve for the low-temperature magnetic flux creep. The self-organized criticality model does not introduce the electrical field  $E$  explicitly. Therefore, we have to extend the above model relating the field  $E$  to a certain characteristics of the model.

When a stable critical state is established, the magnetic flux redistribute inside the sample keeping the critical current density  $j_c$  almost constant. According to the Faraday law a varying magnetic field generates an electrical field  $E$ . The higher is the ramp rate  $h$  of the magnetic field, the higher is an electrical field. We assume here that the dependence between  $E$  and  $h$  is linear, *i.e.*,  $E \propto h$ . We demonstrate in Fig. 6 how an asymptotic current density  $j$  is established for several values of the magnetic field ramp rate  $h$ . In Fig. 7 is shown the dependence of  $E \propto h$  on the asymptotic value of  $j$ , which is an analog of a  $j$ - $E$  curve of Bean's critical state. This logarithmic  $j$ - $E$  curve is consistent with Eq. (3) and numerous experimental data<sup>24</sup>.

## VI. SUMMARY

We demonstrate that an extremal Robin Hood type model evolves to a Been's type critical state. The distribution function of the current density  $G(j)$  in this self-organized state was obtained by numerical simulations as well as analytically. We found that  $G(j)$  has a characteristic cut off at the critical current density. We map the low-temperature magnetic flux creep process to dynamics of an extremal model with Been's type critical state to treat magnetic flux penetration into a superconductor and derive an analog of the current-voltage characteristics in the flux creep regime.

## Acknowledgments

This research was supported by The Israel Science Foundation (grant No. 283/00-11.7).

- 
- \* mints@post.tau.ac.il; <http://star.tau.ac.il/~mints>
- <sup>1</sup> P. G. de Gennes, *Superconductivity of metals and alloys* (W. A. Benjamin, New York, 1966).
  - <sup>2</sup> A. M. Campbell and J. E. Ivett, *Critical currents in superconductors* (Taylor and Francis, London, 1972).
  - <sup>3</sup> C. P. Bean, Phys. Rev. Lett. **8**, 250 (1962).
  - <sup>4</sup> P. W. Anderson, Phys. Rev. Lett. **9**, 309 (1962).
  - <sup>5</sup> P. W. Anderson and Y. B. Kim, Rev. Mod. Phys. **36**, 39 (1964).
  - <sup>6</sup> P. Bak, *How nature works - the science of self-organized criticality* (Copernicus, New York, 1996).
  - <sup>7</sup> H. J. Jensen, *Self-organized criticality - emergent complex behaviour in physical and biological systems* (Cambridge University Press, Cambridge, 1998).
  - <sup>8</sup> E. Altshuler and T.H. Johansen, Rev. Mod. Phys. **76**, 471 (2004).
  - <sup>9</sup> S. I. Zaitsev, Physica A **189**, 411 (1992).
  - <sup>10</sup> Z. Wang and D. Shi, Solid State Commun. **90**, 405 (1994).
  - <sup>11</sup> W. Pan and S. Doniach, Phys. Rev. B **49**, 1192 (1994).
  - <sup>12</sup> S. Field, J. Witt, F. Nori and X. Ling, Phys. Rev. Lett. **74**, 1206 (1995).
  - <sup>13</sup> C.M. Aegerter, Phys. Rev. E **58**, 1438 (1998).
  - <sup>14</sup> K. Behnia, C. Capan, D. Mailyly, and B. Etienne, Phys. Rev. B **61**, R3815 (2000).
  - <sup>15</sup> R. Mulet, R. Cruz and E. Altshuler, Phys. Rev. B **63**, 094501 (2001).
  - <sup>16</sup> C.M. Aegerter, M.S. Welling, and R.J. Wijngaarden, Europhys. Lett. **65**, 753 (2004).
  - <sup>17</sup> L. I. Glazman, N. Ya. Fogel, Fiz. Nizk. Temp. **10**, 95 (1984) [Sov. J. Low Temp. Phys. **10**, 51 (1984)].
  - <sup>18</sup> M. R. Beasley, R. Labusch, and W. W. Webb, Phys. Rev. **181**, 682 (1969).
  - <sup>19</sup> I. Aranson, A. Gurevich, M. S. Welling, R. J. Wijngaarden, V. K. Vlasko-Vlasov, V. M. Vinokur, and U. Welp, cond-mat/0407490 (2004).
  - <sup>20</sup> R. G. Mints and A. L. Rakhmanov, Rev. Mod. Phys. **53**, 551 (1981).
  - <sup>21</sup> M. P. A. Fisher, Phys. Rev. Lett. **61**, 1415 (1989).
  - <sup>22</sup> A. I. Larkin and Yu. N. Ovchinnikov, Zh. Eksp. Teor. Fiz. **65**, 1704 (1973) [Sov. Phys. JETP **38**, 854 (1973)].
  - <sup>23</sup> M. V. Feigelman, V. B. Geshkenbein, A. I. Larkin, and V. M. Vinokur, Phys. Rev. Lett. **63**, 2303 (1989).
  - <sup>24</sup> See A. Gurevich and H. Küpfer, Phys. Rev. B **48**, 6477 (1993) and the references therein.